Autonomous vision-guided bi-manual grasping and manipulation

Alireza Rastegarpanah[1] Naresh Marturi[1,2] Rustam Stolkin[1]

***Abstract*—This paper describes the implementation, demonstration and evaluation of a variety of autonomous, vision-guided manipulation capabilities, using a dual-arm Baxter robot. Initially, symmetric coordinated bi-manual manipulation based on kinematic tracking algorithm was implemented on the robot to enable a master-slave manipulation system. We demonstrate the efficacy of this approach with a human-robot collaboration experiment, where a human operator moves the master arm along arbitrary trajectories and the slave arm automatically follows the master arm while maintaining a constant relative pose between the two end-effectors. Next, this concept was extended to perform dual-arm manipulation without human intervention. To this extent, an image-based visual servoing scheme has been developed to control the motion of arms for positioning them at a desired grasp locations. Next we combine this with a dynamic position controller to move the grasped object using both arms in a prescribed trajectory. The presented approach has been validated by performing numerous symmetric and asymmetric bi-manual manipulations at different conditions. Our experiments demonstrated 80% success rate in performing the symmetric dual-arm manipulation tasks; and 73% success rate in performing asymmetric dual-arm manipulation tasks.**

I. Introduction

Despite half a century of study, industrial manipulation with robots remains predominantly constrained to repetitive, pre-programmed motions, with (typically) limited ability to adapt to changing or uncertain situations. Dual-arm, bi-manual manipulation poses additional challenges in comparison with single-arm manipulation, not least the difficult control problems engendered by closed kinematic chains. There are many reasons why dual-arm manipulation may be useful in practice. For example, an object may be too heavy to be lifted by a single arm alone. Alternatively, an object may be so flexible or fragile that it needs to be grasped simultaneously in two locations, so as to avoid bending or breaking the object while moving it. In other case, two arms may manipulate two objects together to achieve an assembly task. Other motivating reasons, cited for the use of dual-arm robots, include: flexibility and stiffness issues; manipulability; and cognitive issues to do with how human workers perceive mechanical co-workers with human-like forms [1]. Robotic dual-arm manipulation has been used and studied for various industrial and domestic applications such as handling of radioactive goods [2], underwater exploration [3], industrial manufacturing [4], part assembly [5], [6], folding laundry [7], etc.

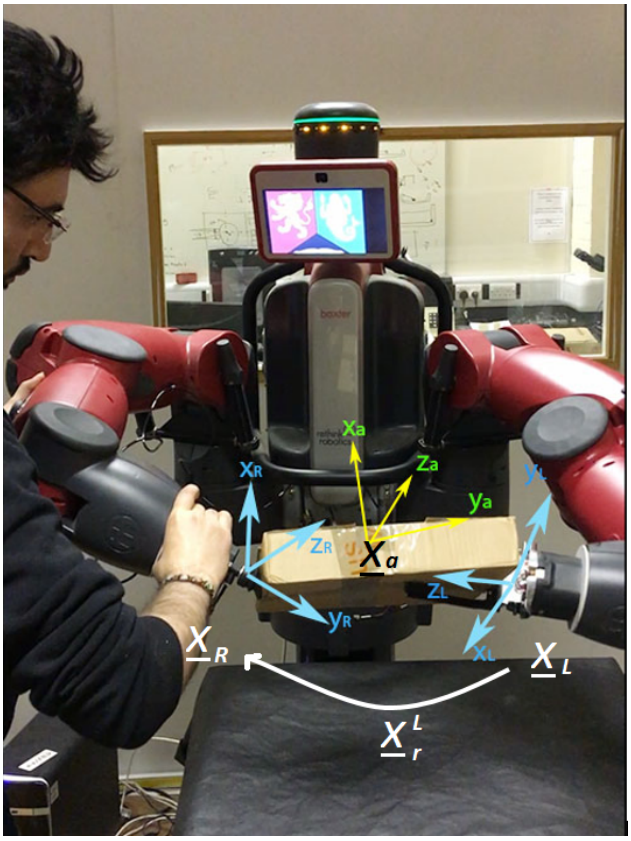

Figure 1. Master-slave manipulation based on task-space approach. The human moves the master arm in arbitrary ways. The slave arm is automatically controlled to maintain a constant transformation between the two end-effectors, thus preserving the bi-manual grasp on the box, regardless of the motions of the arms.

In bi-manual manipulation, a dual-arm robot's two end-effectors interact with the manipulated object, either by holding an object with fixed grasp points [8], or by holding an object by means of frictional interactions with contact points or contact areas [9]. With former, there is no relative motion between the grasping points and in contrast, relative motion may well exists with the latter model, where there may be rolling or sliding contacts between the robot's end-effectors and the grasped object. Typically, force and form closure are not considered in a fixed grasp model, since force closure depends on frictional forces at contact points and form closure properties rely more on friction-less contact models.

Regulation and trajectory tracking are two main problems in control of dual-arm manipulation. In [10], an input-output linearization method was used for trajectory tracking. Hybrid

This work was supported by the EPSRC Feasibility Study project "Machine-learning of vision-guided bi-manual grasps, for adaptable autonomous manipulation in manufacturing environments".

[1]Extreme Robotics Lab, University of Birmingham, Edgbaston, Birmingham, B15 2TT, UK.

[2]Kuka Robotics UK Ltd., Great western street, Wednesbury, WS10 7LL UK.

force/position control was used to control the internal forces at a desirable level based on decomposition between the motion and exerted force control loops [11]. A variety of approaches have been proposed for controlling dual-arm manipulation systems. The symmetric cooperative task-space approach was proposed by Caccavale *et al.* for firm grasp situations, based on internal and external wrenches [12]. Alternatively, manipulation control based on relative and absolute pose was described in [13]. Apart from these, vision-based techniques are being studied recently for accomplishing complex manipulation tasks. Image-based, position-based, and hybrid methods are the three commonly used visual servoing methods for both dual-arm and single arm manipulations. Visual servoing [14] with or without haptic feedback [15] can be used for picking an object when the desired grasping location is known. In [16], an *eye-in-hand* system was used to align the parts held in each hand to be utilized in a dual-arm assembly task. In [17], a real-time adaptive object tracker has been used in conjunction with an optimized visual controller in order to control the joint motions of a 7dof head mechanism, enabling it to track and maintain a prolonged gaze at the objects being manipulated. In [19], a model-based object tracker was used to track an object's pose; in-turn this tracking data was then used by a pose-based visual controller to grasp the objects from known positions.

So far in the literature, two different approaches are commonly used for robotic grasp planning: the first one is based on classical force closure analysis [9] and the second one is based on a direct mapping from vision [18]. In the first method, the magnitude of the external disturbances that a grasp can tolerate will be estimated, by modeling the physical process that are happening at gripper-object interface. Various methods are available based on the latter approach, such as grasp planning by searching for the objects based on gripper stroke, learned stable grasp points [19], etc.

In this paper, we report various experiments investigating the capability of a Baxter robot in performing assorted symmetric and asymmetric coordinated bi-manual tasks. Symmetric tasks are those in which both arms simultaneously manipulate the same object. In contrast, asymmetric tasks describe manipulations in which each arm manipulates a different object or same object at different times. Two different control approaches are presented. The first one is a classical adaptive task space controller, which is based on kinematic tracking algorithm [20] to enable a master-slave manipulation system. The second one includes both joint velocity control and joint position control. An image-based visual controller has been developed to control the joint velocities of both arms to position them at a desired location and to facilitate stable grasping of objects. A dynamic position controller has been developed to move the grasped object along a particular trajectory. Experiments validating the presented approaches are conducted on a bi-manual robot platform, Baxter and the evaluation is performed in terms of accuracy and repeatability of task completion.

The remainder of this paper is structured as follows. In section II we describe various methodologies that are implemented on a Baxter robot to achieve vision-guided bi-manual grasping and manipulative actions. Section III presents our bi-manual manipulation set-up along with a detailed description of the performed tasks and the results obtained with different real-world experiments. Finally, the concluding remarks are provided in section IV.

II. Methodology

In this section, the implemented control approaches for performing coordinated dual-arm manipulation tasks are presented.

A. Dual-arm Manipulation: Task-space Approach

A dual task-space approach has been implemented, based on the configuration between the arms of the Baxter robot and the pose of a coordinate frame set in an object being grasped between the two arms. Fig. 1 shows the tool-centered coordinate frames of the left ($\underline{\mathbf{X}}_R$) and right ($\underline{\mathbf{X}}_L$) end-effectors; and the relative and absolute positions, $\underline{\mathbf{X}}_r^L$ and $\underline{\mathbf{X}}_a$ respectively The relative and absolute positions are defined based on the position of left and right end-effectors and are formulated as follow [12]:

$$\underline{\mathbf{X}}_r^L \triangleq \underline{\mathbf{X}}_L^* \underline{\mathbf{X}}_R \tag{1}$$

$$\underline{\mathbf{X}}_a \triangleq \underline{\mathbf{X}}_L (\underline{\mathbf{X}}_r^L)^{1/2} \tag{2}$$

where, $\underline{\mathbf{X}}_L^*$ is the conjugate of $\underline{\mathbf{X}}_L$ and $(\underline{\mathbf{X}}_r^L)^{1/2}$ is the transformation corresponding to half of the angle ϕ_r around the axis $\mathbf{n}_r^L = in_x + jn_y + kn_z$ of the quaternion $p(\underline{\mathbf{X}}_r^L)$ and half of the translation between the two arms. In this study, the task of manipulating a cardboard box using both arms was tested as illustrated in Fig. 1. The movement of the box is defined relative to a frame (O) located in the robot's torso, while the relative position should remain constant throughout the task. A sequence of unit dual quaternion multiplications has been used to represent the sequence of rigid motions. As shown in Fig. 1, the kinematic tracking algorithm [20] has been used to enable a master-slave manipulation system, where one of the arms tracks the movements of another arm while the relative pose between the two end-effectors remains constant. This concept can be used for industrial applications, e.g. a human collaborating with a robot to handle heavy loads.

B. Dual arm manipulation using Image-based visual control

In this section, we first present an image-based visual servoing scheme to control the motion of both master and slave arms based on the information gained from the visual tracking of a static object. At the end of this step, the two arms are positioned in such a way that the object is tightly held between them. Next, we present an adaptive control strategy to move the grasped object in a desired trajectory. We use the integrated Baxter arm cameras for object detection and visual tracking. It is worth mentioning that the camera

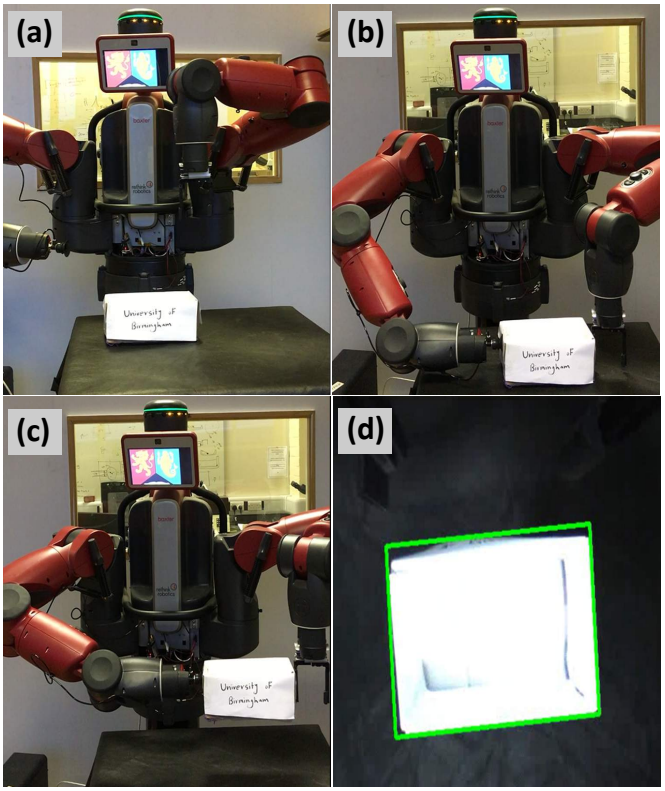

Figure 2. Dual-arm manipulation: (a) robot actively searching to detect the contour of the object, (b) stable grasping using both arms, (c) moving the box along the desired trajectory, (d) detected box during segmentation of the image captured by the wrist camera. See supplementary video for clear illustration.

intrinsics are estimated beforehand using classical calibration approach [21]. The pixel values of the scene are mapped to the Baxter robot coordinates as given by (3):

$$O = (P_p C_p) * C_c * d + B_p + G_o \tag{3}$$

where, $O, P_p, C_p, O_p, G_o, C_c$ and d represent Baxter coordinates, pixel coordinates, centre pixel coordinates, Baxter pose, gripper offset, camera calibration factor and distance from the table respectively. Since, no depth estimation has been used in this work, the distance from the robot to the object is pre-fixed.

The task is initialised by placing a box on the table as shown in Fig. 2a. The robot then moves its left wrist camera over the table in order to detect the box and segment it from the image. For this task, we assume that the left arm is master. The Canny Edge Detector technique has been used to find the edges of the object with low error rate, good localization and minimal response. The Gaussian filter is used in order to remove the noise of the captured image, to avoid false edge detection caused by noise. Next, additional non-edge pixels are removed by applying non-maximum suppression. Finally, the edge is accepted or rejected by applying upper and lower threshold for a pixel gradient. This process enables us to find a bounding box of the object as shown in Fig. 2d. The robot continues with active searching if the desire bounded region is not found. The orientation of the box has been estimated with respect to the coordinates of the corners and centroid of the object.

Once the initial bounding region of the target object (white box in Fig. 2) is detected, visual tracking starts automatically. In this work, we use a particle filter-based tracker to provided arm control feedback. Initially detected bounding region has been used as the reference region for the tracker in first iteration and a reference model Ψ_r has been computed using individual channel histograms *i.e.,* in *rgb* space. Next, uniformly sampled candidate regions are allocated around the reference and their individual models are computed Ψ_i, where i is the individual candidate index. The best candidate i.e., the region enclosing our object, has been computed by finding the maximum of vector of Bhattacharya coefficients computed between the reference model and each individual candidate model. The coefficient ρ_i for candidate region i is computed using

$$\rho_i = \sqrt{\Psi_r \Psi_i} \tag{4}$$

The corresponding region with the maximum coefficient value is retained and propagated as a reference region to the next frame. The centroid of this region is used as a feedback in controlling the velocity of the robot arm. The desired point to reach *i.e.,* the reference feature $\mathbf{P}^*$ has been pre-learned and the centroid point $\mathbf{P}_c$ from previous step is used as observed features. Using these two, the task space error $\mathbf{e} = \mathbf{P}^* - \mathbf{P}_c$ to regulate has been framed. Although, this can be regulated using a classing visual controller [22], in order to have optimised performance, in this work we use the control law inspired from Levenberg-Maquardt optimization, which is given by equation (5)

$$\mathbf{v} = \lambda \left(\mathbf{J}^\top \mathbf{J} + \mu \left(\mathbf{J}^\top \mathbf{J}\right)\right)^{-1} \mathbf{J}^\top \mathbf{e} \tag{5}$$

where, $\lambda < 0$ and $\mu > 0$ are gain values, $\mathbf{v}$ is robot joint velocities and $\mathbf{J}$ is the robot Jacobian in task space computed using (6)

$$\mathbf{J} = \mathbf{L}\,\mathbf{V}_e\,\mathbf{J}_b \tag{6}$$

where, $\mathbf{L}$ is the image space space Jacobian computed using observed centroid features, $\mathbf{V}_e$ is the velocity twist matrix, and $\mathbf{J}_b$ is robot joint space Jacobian computed using forward kinematics. The control law given in (5) drives the left robot arm (master) to position arm's end-effector supporting one side of the task object. An important point to note here is that the the desired goal position for the robot to reach has been selected with an offset above the original goal point along the camera optical axis. This is due to the fact that the camera field of view reduces while the robot moves towards the object, which leads to failures in target tracking. Hence, when the robot reaches the pre-fixed goal, it simply moves down in a straight line path compensating the offset. Now, similar to the task space approach described in previous section, the second arm is commanded using kinematic tracking algorithm *i.e.,* the second arm moves in the mirrored space of the master arm.

Once the two arms are positioned at their desired locations, the dual-arm manipulation trajectory control starts automatically. In this study, an adaptive control scheme has been used to control and manipulate the movement of an object along a desired trajectory. The object has been modeled as a mass-spring-damper system. The dynamics model of the object are formulated according to (7) [23]:

$$\begin{bmatrix} F_L \\ F_R \end{bmatrix} = \begin{bmatrix} k & d \\ k & d \end{bmatrix} \begin{bmatrix} X_m \\ \dot{X}_m \end{bmatrix} + \begin{bmatrix} -k & 0 & -d & 0 \\ 0 & -k & 0 & -d \end{bmatrix} \begin{bmatrix} X_L \\ X_R \\ \dot{X}_L \\ \dot{X}_R \end{bmatrix} + \begin{bmatrix} kl \\ -kl \end{bmatrix} \quad (7)$$

where, F_L and F_R represent the interaction forces at left and right arm, X_L and X_R are Cartesian position of left and right arm, $\dot{X}_L$ and $\dot{X}_R$ represent the Cartesian velocity of left and right arm, and m, k, d represent object mass, stiffness and damping, respectively. The dynamics of the robot are modeled as follows:

$$M_L(q_L)\ddot{q}_L + C_L(q_L, \dot{q}_L)\dot{q_L} + G_L(q_L) = \tau_{uL} + f_L \quad (8)$$

$$M_R(q_R)\ddot{q}_R + C_R(q_R, \dot{q}_R)\dot{q_R} + G_R(q_R) = \tau_{u_R} + f_R \quad (9)$$

where, M_L and M_R represent symmetric bounded positive definite inertia matrix for the left and right arm respectively, q_L and q_R represent joint position for the left and right arm respectively, $C_{L,R}(q, \dot{q})\dot{q}$ represent the Coriolis and Centrifugal force, $C_{L,R}(q)$ is the gravitational force, $\tau_{u_{L,R}}$ represent the vector of control input torques and $f_{L,R}$ represent the external force created by friction or load. The desired trajectory was defined in Cartesian space for the left arm (master) and then the trajectory for the right arm was formulated with respect to a desired offset from the left arm. The desired trajectory of the master and slave arms are formulated based on a starting point $(y^*(0))$ and a desired destination point $(y^*(T))$ with T being the period of the trajectory, as follows:

$$X_L^*(0) = [x_L(0), y_L^*(t), z_L(0), \vartheta_L(0), \phi_L(0), \psi_L(0)]^T \quad (10)$$

$$X_R^*(t) = [x_L(t), (y_L(t) + \underline{\mathbf{X}}_r^L), z_L(t), \vartheta_L(t), \phi_L(t), \psi_L(t)]^T \quad (11)$$

where $\underline{\mathbf{X}}_r^L$ shows the relative pose (explained in previous section) and $z_L(t), \vartheta_L(t), \phi_L(t)$, and $\psi_L(t)$ are determined by calculating the forward kinematics of the left arm. The control law to move the box along a desired trajectory is then given by

$$\tau_u(t) = \mathbf{J}^T(q) F_x kd \quad (12)$$

where, $\mathbf{J}(q)$ is the Jacobian and $F_x kd$ represents the sum of forces. As shown in Fig. 2b, the left arm was moved to the left side of the box and right arm with suction cap was moved to the right side of the box. Next, the relative pose was set to be the length of the box, after which the box could be lifted and moved to the desired destination position by using the dual-arm task space technique (Fig. 2c). The trajectory tracking error $\varepsilon(t)$ was calculated by (13):

$$\varepsilon(t) = \dot{e}(t) + ke(t) \quad (13)$$

where, $e(t)$ and $\dot{e}(t)$ are the joint errors, calculated respectively from (14) and (15) as follow:

$$e(t) = q(t) - q^*(t) \quad (14)$$

$$\dot{e}(t) = \dot{q}(t) - \dot{q}^*(t) \quad (15)$$

Two levels of collision avoidance were implemented within all algorithms during all experiments. The first collision detection was performed through visualizing the robot in RVIZ software. The second level of protection deals with impact and "squish", when sudden changes in joint torques are detected, or when any applied torque is greater than a pre-defined threshold.

III. Experimental Validations

A. Experimental Set-up

The experimental setup used in this work consists of a bi-manual robot, Baxter equipped with a parallel jaw gripper on the left hand and a suction gripper on the other hand. The compressor pressure (of the suction gripper) was maintained constant on 6 psi during all the experiments. The vision system includes two single cameras that are integrated within each arm (located at the end-effector) and can provide images with a framerate of $\sim$ 25 fps. The task space contains a table covered with black cloth (to reduce the light reflections) placed in front of the robot. Four different objects are used for the experiments: a cardboard box, rectangular and circular foams, and light weight indoor golf balls. The communication with the robot controller, cameras and work computer (4.00 GHz Intel Core i7 CPU with 8 Gb of RAM) has been realized through the latest version of ROS framework.

B. Studied Tasks

In this study, the capability of Baxter in performing various dual-arm tasks has been evaluated by conducting various experiments including symmetric and asymmetric manipulations. In the 1st experiment, adaptive task space control system was used in order to move a box along the created trajectory. Here the master arm was moved by a human operator, thus, creating an arbitrary trajectory for the slave arm to follow (Fig. 1). This test was performed to show the proof of principle of kinematic tracking algorithm. Then, this concept was extended to perform symmetric coordinate manipulation tasks using image-based visual servoing. Adaptive control system was used to move a box along a predefined trajectory using both arms (Fig. 2). The protocol of 2nd experiment was to detect a cylindrical foam, grasp the object with parallel jaw gripper, move the left arm to the predefined position and finally grasp the object using suction gripper of other hand (Fig. 7). In the last experiment, the task was to detect the rectangular foam first, and then detect the yellow balls. At

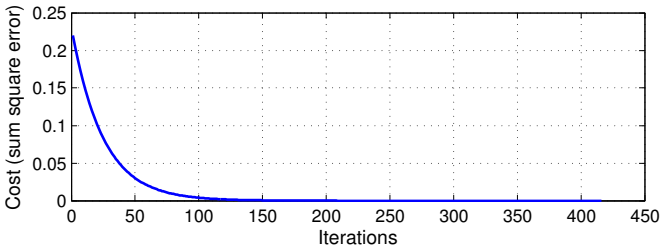

Figure 3. Cost (sum squared error, $\mathbf{e}$) variation with image-based visual servoing while positioning the master arm at the side of the cardboard box.

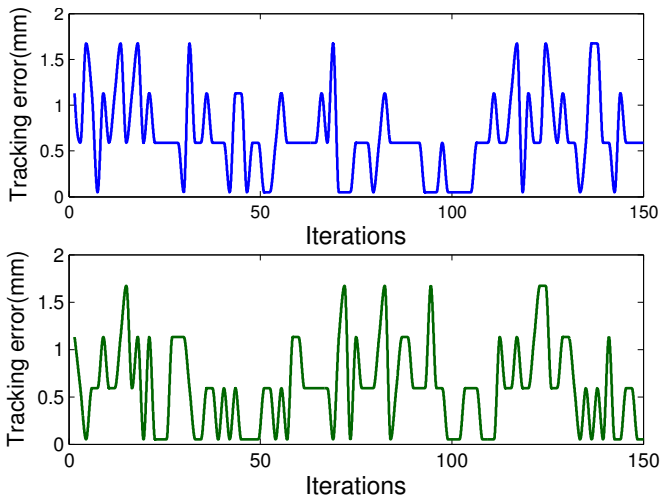

Figure 4. Norm of tracking error during dual-arm symmetric manipulation (top) Left arm, (bottom) Right arm

the end, the robot has to grasp and place the balls at the centre of the rectangular foam (Fig. 9).

C. Symmetric dual-arm manipulation

The task is initialised by detecting the bounding region of the box $(30cm \times 20cm \times 15cm)$ as shown in Fig. 2(d), then the left arm was visually servoed to reach the left side of the box. Fig. 3 shows the cost variation *i.e.,* the sum squared error $\mathbf{e}$ during the positioning process. The trajectories of the right and left arms were defined and then task space adaptive control was used to move the object with respect to the relative pose. Fig. 4a and Fig. 4b show respectively the tracking error norms (computed using (13) - (15)) of the left arm and right arm. The experiment has been repeated for 30 different trials and each trial took 41s in average. Fig. 5 illustrates the performance over all trials. From the obtained results it can be seen that the success rate is %80, which demonstrates the robustness of the system in performing the bi-manual manipulation task by using our implemented adaptive control scheme. The task failed once due to incorrect detection of edges by the vision system, most likely due to light reflections. Another source of failure is the collision. Two different collisions are noted, the arm colliding with the box and with the table.

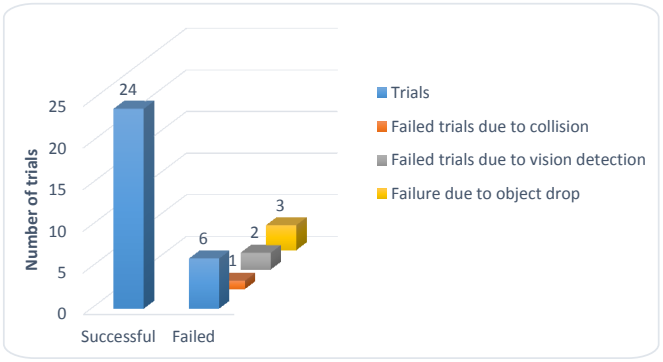

Figure 5. Success rate of performing the symmetric coordinated dual-arm manipulation task using task-space adaptive control.

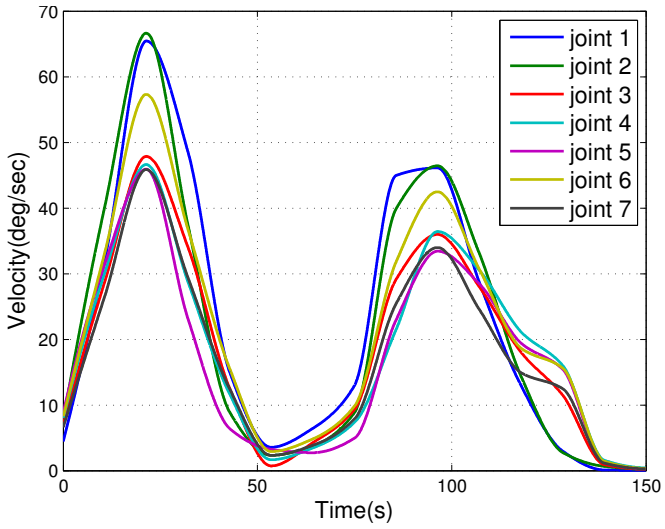

Figure 6. Joint velocities of left arm during picking the object.

D. Asymmetric dual-arm manipulation

In this section, we explored the possibilities of using robots in industry to perform various bi-manual tasks such as assembly/dismantle, pick and place, and robot-human collaborative tasks. For the sake of demonstration, we use a cylindrical deformable object $(5cm \times 3cm)$, which has been detected in the images from left arm's camera using the Hough transformation for circle detection. More complex shapes can also be robustly detected, by using advanced algorithms from the vision literature. However, the underlying robot control principles (the focus of this paper) would remain same. The robot arms are commanded as described in the section II. The velocities of the left arm joints have been recorded and are shown in Fig. 6. The robot's last three joints are capable of attaining maximum speeds of $4rad/s$ (230 degrees/s). However, our experiments were performed at low velocities and the maximum recorded joint velocity was 66 degrees/s. As shown in Fig. 7a, the robot actively searches for the object by moving the left camera. After detecting the object and segmenting the object's perimeter, the robot was commanded to reach the desired grasping location and grasp the object.

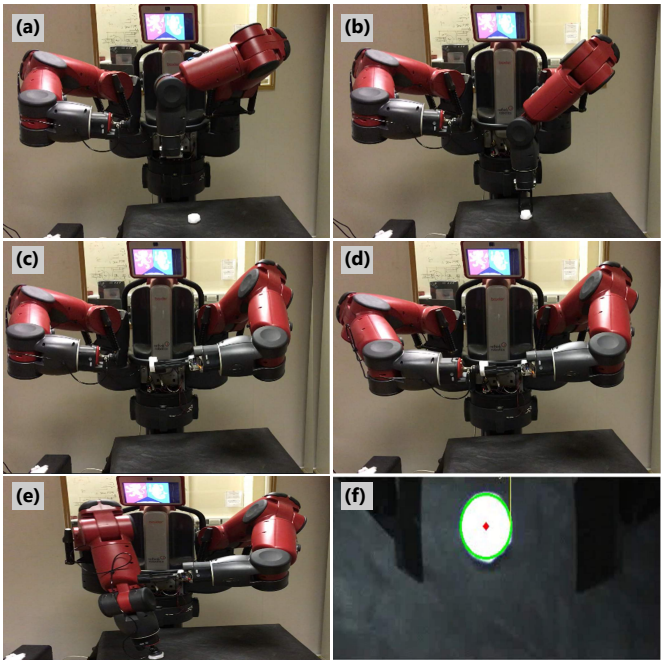

Figure 7. Asymmetric dual-arm manipulation - handoff of object from left arm to right arm: (a) and (b) searching, detecting and grasping the object, (c) moving the left arm to the hand-over position, (d) grasping the object by the right arm, (e) placing the object on the target position, (f) visually detecting the contour and object centroid. See supplementary video for clear illustration.

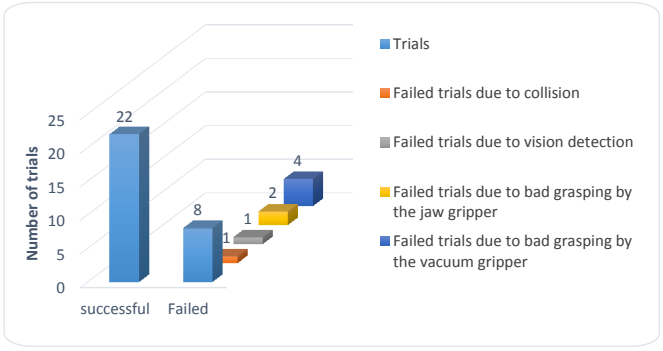

Figure 8. Success rate of performing the asymmetric coordinated dual-arm manipulation task using velocity control.

The center point of the parallel jaw gripper is positioned to be coincident with the center position of the detected object (Fig. 7b). Finally, the right arm is moved to a position (Fig. 7c) such that it can grasp the object from the left arm (figure7d) and place it on a desired destination position on the table (Fig. 7e). This experiment was repeated over 30 trials and each trial took 45s in average. The task performance is shown in Fig. 8. In this experiment, the success rate was %73 with 8 failed trials. Six of these failures were due to a sudden pressure change in the compressor causing a failure of the vacuum gripper. In just two trials, the center point of the object was not calculated correctly by the vision system, and the robot was therefore not able to grasp the object correctly. With respect to the presented setup for both symmetric/asymmetric

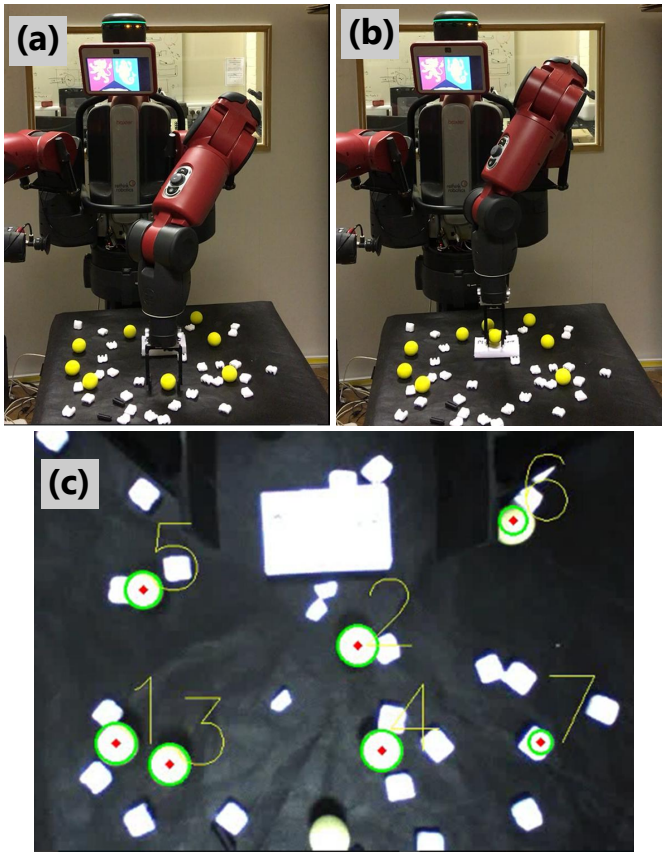

Figure 9. Single arm manipulation in cluttered scenes: (a) detecting the white box and yellow balls, (b) grasping a ball and placing it on the white box, (c) detected objects, automatically labeled in order of which object is to be grasped first. See supplementary video for clear illustration.

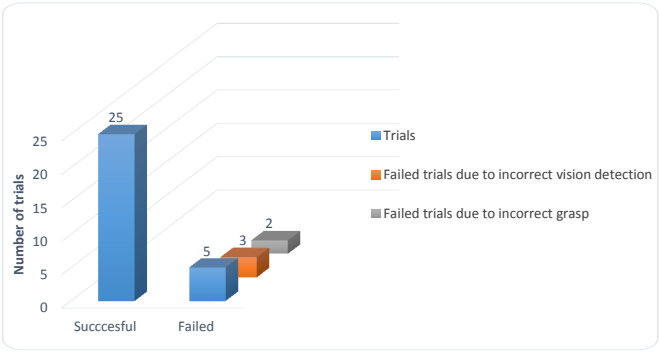

Figure 10. Success rate of performing single-arm manipulation task.

dual-arm manipulation tasks, the scenario can be replicated by another party in order to replicate and improve the tasks.

E. Single Arm Manipulation: Grouping of Objects

This test has been performed as an extension to the previous experiment, where we demonstrate the task of grouping objects within a cluttered scene. The objects to be detected and grasped are yellow balls, with diameter of 4cm, where the task is to place them on top of a rectangular box. It is worth mentioning that this last test uses only one arm

(master) and hence, the complexity of manipulation is less than the other two experiments. Similar to the previous experiments, an active search is performed initially to detect yellow balls in the scene. The balls are labeled accordingly as shown in Fig. 9c so as to plan their placement on top of the box. The location of box (in robot frame) is known beforehand. Similar to previous, this test has been repeated 30 times and the task performance is shown in Fig. 10. Task of collecting 7 balls in each trial took about 36s in average. In [24], the single grasping success rate for the previously seen objects was %73, while the corresponding rate was %83 in this study. Also result demonstrates %7 higher success rate for the symmetric dual-arm manipulation task than asymmetric dual-arm manipulation. It is worth mentioning, as the number of trials increases, the success rate might be decreased due to random failures. In this study, failures caused mainly by vision system and grippers which both of them can be improved by using new object detection techniques, like Scalable Tree-based approach for joint object and pose recognition in 3D or detection-based object labeling in 3D scenes, and utilizing robust grippers with higher precision.

IV. Conclusion

In this study, a variety of manipulation tasks have been attempted, using a dual-arm Baxter robot. In this study we obtained promising results which suggest the capability of Baxter to be used for light industrial applications, with particular potential for safely collaborating with humans. The success rate of %80 shows the high capability of the robot in performing dual-arm manipulation tasks. Collision, incorrect vision detection and weak grasping were three main reasons for the small number of task failures recorded in this study. Our ongoing work is extending these methods to explore dual-arm manipulation applications with a pair of industrial-quality KUKA LBR iiwa robots, using more complex hands and sensors, and more sophisticated and robust grasp planning algorithms in order to generalize these manipulation tasks to real-world environments.

References

[1] C. Smith, Y. Karayiannidis, L. Nalpantidis, X. Gratal, P. Qi, D. V. Dimarogonas, and D. Kragic, "Dual arm manipulationâĂŤa survey," *Robotics and Autonomous systems*, vol. 60, no. 10, pp. 1340–1353, 2012.

[2] T. I. Burrell, A. Montazeri, S. D. Monk, and C. J. Taylor, "Feedback control-based inverse kinematics solvers for a nuclear decommissioning robot," in *7th IFAC Symposium on Mechatronic Systems*, 2016.

[3] E. J. Hanly, M. R. Marohn, S. L. Bachman, M. A. Talamini, S. O. Hacker, R. S. Howard, and N. S. Schenkman, "Multiservice laparoscopic surgical training using the davinci surgical system," *The American Journal of Surgery*, vol. 187, no. 2, pp. 309–315, 2004.

[4] J. Krüger, G. Schreck, and D. Surdilovic, "Dual arm robot for flexible and cooperative assembly," *CIRP Annals-Manufacturing Technology*, vol. 60, no. 1, pp. 5–8, 2011.

[5] A. Marturi, "Vision based grasp planning for robot assembly," *International MasterâĂŹs Thesis, Orebro University*, 2010.

[6] Y. Yamada, S. Nagamatsu, and Y. Sato, "Development of multi-arm robots for automobile assembly," in *Robotics and Automation, 1995. Proceedings., 1995 IEEE International Conference on*, vol. 3. IEEE, 1995, pp. 2224–2229.

[7] K. Salleh, H. Seki, Y. Kamiya, and M. Hikizu, "Inchworm robot grippers in clothes manipulationâĂŤoptimizing the tracing algorithm," in *Intelligent and Advanced Systems, 2007. ICIAS 2007. International Conference on*. IEEE, 2007, pp. 1051–1055.

[8] A. Bicchi, "Hands for dexterous manipulation and robust grasping: A difficult road toward simplicity," *IEEE Transactions on robotics and automation*, vol. 16, no. 6, pp. 652–662, 2000.

[9] A. Bicchi and V. Kumar, "Robotic grasping and contact: A review," in *ICRA*. Citeseer, 2000, pp. 348–353.

[10] X. Yun and V. R. Kumar, "An approach to simultaneous control of trajectory and interaction forces in dual-arm configurations," *IEEE Transactions on Robotics and Automation*, vol. 7, no. 5, pp. 618–625, 1991.

[11] D. Navarro-Alarcon, V. Parra-Vega, S. Vite-Medecigo, and E. Olguin-Diaz, "Dexterous cooperative manipulation with redundant robot arms," in *Iberoamerican Congress on Pattern Recognition*. Springer, 2009, pp. 910–917.

[12] F. Caccavale, P. Chiacchio, and S. Chiaverini, "Task-space regulation of cooperative manipulators," *Automatica*, vol. 36, no. 6, pp. 879–887, 2000.

[13] B. V. Adorno, "Two-arm manipulation: From manipulators to enhanced human-robot collaboration," Ph.D. dissertation, Université Montpellier II-Sciences et Techniques du Languedoc, 2011.

[14] N. Marturi, A. Rastegarpanah, C. Takahashi, R. Stolkin, J. Kuo, and Y. Bekiroglu, "Towards advanced robotic manipulation for nuclear decommissioning: A pilot study on tele-operation and autonomy," in *IEEE International Conference on Robotics and Automation for Humanitarian Applications*, in-press.

[15] A. Petrovskaya, O. Khatib, S. Thrun, and A. Y. Ng, "Bayesian estimation for autonomous object manipulation based on tactile sensors," in *Proceedings 2006 IEEE International Conference on Robotics and Automation, 2006. ICRA 2006.* IEEE, 2006, pp. 707–714.

[16] V. Lippiello, B. Siciliano, and L. Villani, "An experimental setup for visual servoing applications on an industrial robotic cell," in *Proceedings, 2005 IEEE/ASME International Conference on Advanced Intelligent Mechatronics.* IEEE, 2005, pp. 1431–1436.

[17] N. Marturi, V. Ortenzi, J. Xiao, M. Adjigble, R. Stolkin, and A. Leonardis, "A real-time tracking and optimised gaze control for a redundant humanoid robot head," in *Humanoid Robots (Humanoids), 2015 IEEE-RAS 15th International Conference on*. IEEE, 2015, pp. 467–474.

[18] C. Bard and J. Troccaz, "Automatic preshaping for a dextrous hand from a simple description of objects," in *Intelligent Robots and Systems' 90.'Towards a New Frontier of Applications', Proceedings. IROS'90. IEEE International Workshop on*. IEEE, 1990, pp. 865–872.

[19] A. Saxena, J. Driemeyer, and A. Y. Ng, "Robotic grasping of novel objects using vision," *The International Journal of Robotics Research*, vol. 27, no. 2, pp. 157–173, 2008.

[20] L. Figueredo, B. V. Adorno, J. Y. Ishihara, and G. Borges, "Switching strategy for flexible task execution using the cooperative dual task-space framework," in *2014 IEEE/RSJ International Conference on Intelligent Robots and Systems*. IEEE, 2014, pp. 1703–1709.

[21] R. Tsai, "A versatile camera calibration technique for high-accuracy 3d machine vision metrology using off-the-shelf tv cameras and lenses," *IEEE Journal on Robotics and Automation*, vol. 3, no. 4, pp. 323–344, 1987.

[22] V. Ortenzi, N. Marturi, R. Stolkin, J. Kuo, and M. Mistry, "Vision-guided state estimation and control of robotic manipulators which lack proprioceptive sensors," in *IEEE/RSJ International Conference on Intelligent Robots and Systems*, in-press.

[23] A. Smith, C. Yang, H. Ma, P. Culverhouse, A. Cangelosi, and E. Burdet, "Biomimetic joint/task space hybrid adaptive control for bimanual robotic manipulation," in *11th IEEE International Conference on Control & Automation (ICCA)*. IEEE, 2014, pp. 1013–1018.

[24] L. Pinto and A. Gupta, "Supersizing self-supervision: Learning to grasp from 50k tries and 700 robot hours," *arXiv preprint arXiv:1509.06825*, 2015.